International Journal of Mechanical, Industrial and Aerospace Sciences
ISSN: 2517-9950
Vol:3, No:2, 2009

Flow Characteristics Impeller Change of an Axial Turbo Fan

Young-Kyun Kim, Tae-Gu Lee, Jin-Huek Hur, Sung-Jae Moon, and Jae-Heon Lee

***Abstract*—**In this paper, three dimensional flow characteristic was presented by a revision of an impeller of an axial turbo fan for improving the airflow rate and the static pressure. T_O consider an incompressible steady three-dimensional flow, the RANS equations are used as the governing equations, and the standard k-ε turbulence model is chosen. The pitch angles of 44°, 54°, 59°, and 64° are implemented for the numerical model. The numerical results show that airflow rates of each pitch angle are 1,175 CMH, 1,270 CMH, 1,340 CMH, and 800 CMH, respectively. The difference of the static pressure at impeller inlet and outlet are 120 Pa, 214 Pa, 242 Pa, and 60 Pa according to respective pitch angles. It means that the 59° of the impeller pitch angle is optimal to improve the airflow rate and the static pressure.

***Keywords*—**Axial turbo fan, Impeller, Blade, Pitch angle.

I. Introduction

THE axial fan is the fluid machinery which was used for aeration, exhaustion, and ventilation. Small-sized fans are applied to the home electronics and automobile engines etc. Large-sized fans are adopted for the ventilation of the factory, and tunnerls.[1] The axial turbo fan has been recently used in the hotel lobby, the large scale interior gymnasium, and museum to prevent the stratification of the temperature field on the ceiling. Eventually this improves the aeration efficiency. In order to increase the arrival distance of blown air from the axial turbo fan, the impeller that can have high air flow rate and statistic pressure is necessary for the efficient application of a turbo fan.

In order to increase the flow rate and the static pressure of the impeller it is necessary to suggest the optimal design shape of a blade by experimental examination. Until now we have used simple experienced cut-and-try method or 2 dimensional mathematical calculation to satisfy the design parameters such as flow rate, static pressure rise, and efficiency. Since this method can not show the complicated flow behavior and pressure distribution we should make a prototype of a fan to guarantee the maxmum flow rate and static pressure increase. In order to overcome the disadvantage of a model test, this requires lots of time and cost the direct analysis of flow field the fan is widely used via computational fluid dynamics based on RANS(Reynolds Averaged Navier-Stokes) equations.[2],[3]

In this study, numerical analysis is used to investigate the effect of pitch angle variation on the flow rate and the static pressure to suggest the design parameters for a turbo fan which has 250 Pa and 1,400 CMH.

Young-Kyun Kim is with the [1]Department of Mechanical Engineering, Graduate School of Hanyang University, Seoul 133-791, Korea (e-mail: sohgo@hanmail.net)

Tae-Gu Lee is with the Plant Division of Hyun-Dai,, Seoul 110-920, Korea (e-mail: leetg0704@hdec.co.kr)

Jin-Huek Hur is with the [1]Department of Mechanical Engineering, Graduate School of Hanyang University, Seoul 133-791, Korea (e-mail: mlg20@hanmail.net)

Sung-Jae Moon is with the [1]Department of Mechanical Engineering, Hanyang University, Seoul 133-791, Korea (e-mail: gregmoon@hanmail.net)

Jae-Heon Lee is with the [1]Department of Mechanical Engineering, Hanyang University, Seoul 133-791, Korea (corresponding author to provide phone:82-02-2220-0425;fax:82-02-2220-4425; e-mail: jhlee@hanyang.ac.kr).

II. The Shape of Impeller

Fig. 1 shows the front view, the profile, and the section of an impeller wing. The impeller is composed of a hub and the blades. The end of an wing is tip. In Fig. 1(a) the hub diameter of the impeller, D_H is 202 mm and the entire diameter of the impeller, D_I is 110 mm. The thickness of the impeller, T_I is 44 mm. This impeller rotates at the rate of 3,450 rpm, counter-clockwise. Fig. 1(b) represents the cross-section of the airfoil. The angle between the surface of hub and the tip surface is called twist angle, φ . A wing has a pressure side a suction side. Pressure side raises static pressure. And latter takes air flow from the fan entrance and the former raises the static presuure of the flow. The straight line from leading edge to trailing edge is called as "chord". We express the chord length as X_c, which is equal to the chord length in the hub of the impeller blade and the chord length in the tip.

.

TABLE I
Impeller Geometry Parameters

Definition		
D_I	Impeller diameter [mm]	202
D_H	Hub diameter [mm]	110
T_I	Impeller thickness [mm]	44
X_c	Chord length [mm]	37
Y_b	Camber [mm]	1.8
Y_t	Blade thickness [mm]	4.6
ϕ	Twist angle [°]	24
β	Pitch angle [°]	54

The blade thickness Y_t, the camber Y_b, and the pitch angle β determined the shape of a impeller wing together with X_c.[4] Table I suggest other design variables

III. Analysis Method of the Impeller Flow Characteristics

1. Governig equations

When the flow characteristics in the rotating machinery is analysed the relative coordinate system is generally adopted because of convienient application of the steady state and boundary conditions.[5] In this study the relative coordinate system is used to decribe the 3-dimensional incompressible steady flow inside the axial turbo fan.

A continuity equation, momentum equations, and equations for a turbulence model are applied as shown in Table II.[6] The standard k-ε model is used to approximate turbulence.[7] The centrifugal force and Coriolis force by the rotation of

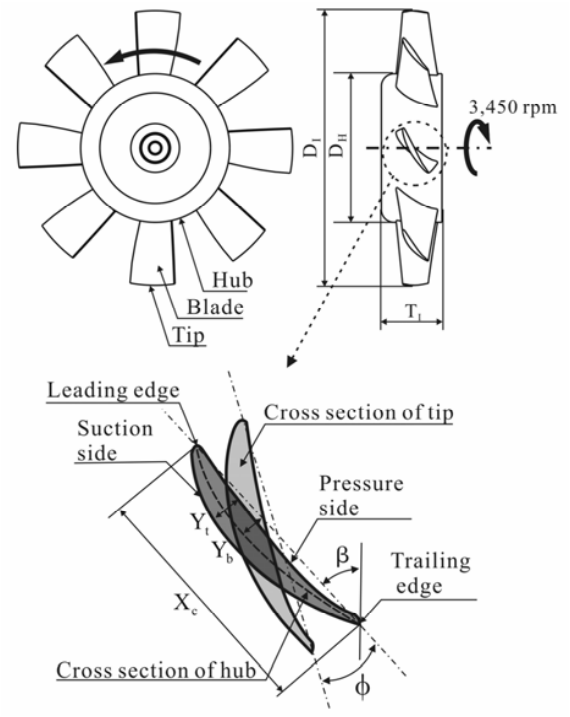

Fig. 1 Schematic diagrams of the impeller in present investigation

coordinate axis appears as the source term, $\vec{B}$ in the momentum equations. The relative velocity formulation with rotation is shown in Fig. 2. $\vec{W}$, $\vec{V}$ and $\vec{U}$ mean the relative velocity, absolute velocity, and rotation velocity. The rotation velocity can be produced by the vector product of angular velocity and the position vector.[8]

$$\vec{W} = \vec{V} + \vec{U} = \vec{V} + (\vec{\omega} \times \vec{r}) \quad (1)$$

2. Analysis field and boundary condition

Fig. 3 depicts the flow field domain to understand the flow characteristic inside the fan. The intake flow by the rotation of the impeller obtains the static pressure rise in passing through the impeller. The flow exits the casing. The length of the solution domain from the casing entrance to the casing entrance to the casing exit is 3 times of the impeller diameter.

By the symmetry, only π /4 domain of a wing is considered since the impeller has 8 wings.

TABLE II
Governing Equations

Continuity equation ;

$$div(\rho \vec{W}) = 0$$

x-momentum equation ;

$$div(\rho w_x \vec{W}) = -\frac{\partial p}{\partial x} + div(\mu\, grad\, w_x) + B_x$$

y-momentum equation ;

$$div(\rho w_y \vec{W}) = -\frac{\partial p}{\partial y} + div(\mu\, grad\, w_y) + B_y$$

z-momentum equation ;

$$div(\rho w_z \vec{W}) = -\frac{\partial p}{\partial z} + div(\mu\, grad\, w_z) + B_z$$

Turbulent kinetic energy equation ;

$$div(\rho k \vec{W}) = div(\frac{\mu_t}{\sigma_k} grad\, k) + G_k - \rho\epsilon$$

Dissipation rate equation of turbulent kinetic energy ;

$$div(\rho \epsilon \vec{W}) = div(\frac{\mu_t}{\sigma_\epsilon} grad\, \epsilon) + C_{1\epsilon} G_k \frac{\epsilon}{k} - C_{2\epsilon}\rho \frac{\epsilon^2}{k}$$

where,

$$\vec{W} = w_x \vec{i} + w_y \vec{j} + w_z \vec{k}$$

$$\vec{B} = B_x \vec{i} + B_y \vec{j} + B_z \vec{k} = -\rho(2\vec{w} \times \vec{W} + \vec{w} \times \vec{w} \times \vec{r})$$

$$\mu_t = \frac{C_\mu \rho k^2}{\varepsilon}\ ,\ G_k = \mu_t(\frac{\partial \omega_i}{\partial x_i} + \frac{\partial \omega_i}{\partial x_j})\frac{\partial \omega_i}{\partial x_i}$$

$C_\mu = 0.09$, $C_{1\varepsilon} = 1.44$, $C_{2\varepsilon} = 1.92$, $\sigma_k = 1.0$, $\sigma_\varepsilon = 0.9$

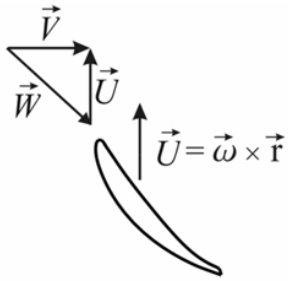

Fig. 2 Schematic diagram for relative velocity formulation

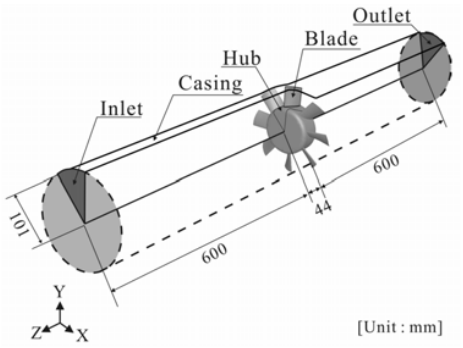

Fig. 3 Solution domain

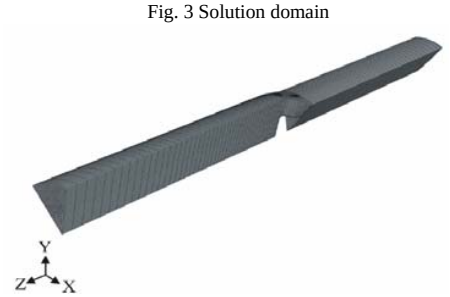

Fig. 4 Computational grid system

The boundary conditions are imposed on the entrance, the outlet, and the wall in casing. No-slip boundary conditions are applied on the impeller wing and the hub. The symmetry cross-section should have periodic boundary conditions. Atmospheric pressure is put on the entrance as the boundary condition. The exit of the casing has the outlet boundary condition. Non-uniform grid system was used. The number of grid points are 120,000 as shown in Fig. 4.

The residue less than 10^{-4} is used as the convergence criteria for each equation in the iteration process. The average number of iterations was about 1,200.

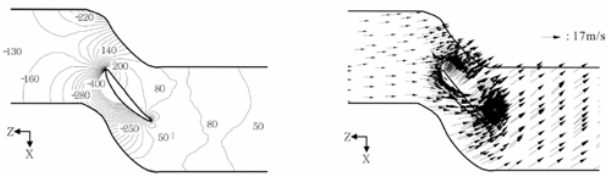

(a) Distribution of static pressure [Pa] (b) Distribution of absolute velocity vectors

Fig. 5 Numerical results on the mid-span plane of 54° pitch angle of impeller blade

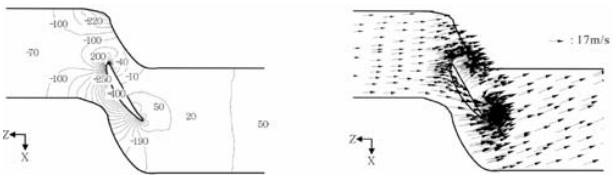

(a) Distribution of static pressure [Pa] (b) Distribution of absolute velocity vectors

Fig. 6 Numerical results on the mid-span plane of 44° pitch angle of impeller blade

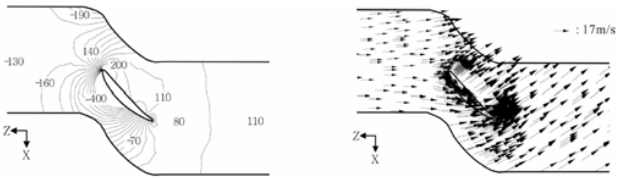

(a) Distribution of static pressure [Pa] (b) Distribution of absolute velocity vectors

Fig. 7 Numerical results on the mid-span plane of 59° pitch angle of impeller blade

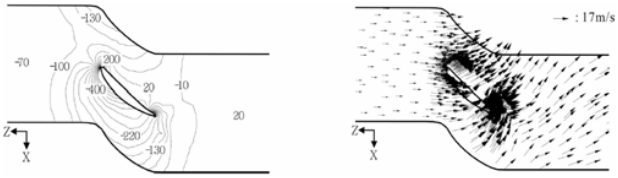

(a) Distribution of static pressure [Pa] (b) Distribution of absolute velocity vectors

Fig. 8 Numerical results on the mid-span plane of 64° pitch angle of impeller blade

IV. Result and Discussion

In this work, the difference of flow characteristics between of the design pitch angles of 54° and of the corrected pitch angles of 44°, 59°, and 64° is investigated.

Fig. 5 shows the static pressure difference of 214 Pa and the flow rate of 1270 CMH with the design pitch angle of 54°. The absolute velocity fields and the pressure distributions at the wing cross-section according to the pitch angle variation are presented from Fig. 5 to Fig. 8.

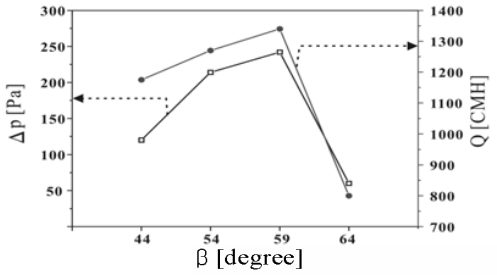

Fig. 9 Pressure difference and air flow rate according to pitch angles

Fig. 6 shows the smallest static pressure difference and the flow rate due to the smallest flow resistance by the pitch angle of 44°.

In Fig. 7, which shows the static pressure distribution and the flow rate with pitch angle of 59°, the pressure difference increased by the increase of the pitch angle. The flow rate increase by the static pressure increase, produces the absolute velocity of 17 m/s at the exit of the impeller. This velocity induces the designed maximum flow rate.

In Fig. 8, which shows the case of pitch angle 64°, the

pressure at the exit is the smallest pressure affected by the negative pressure on the pressure side of the wing due to the large pitch angle of 64°. Because of the recirculation at the exit of the impeller, the flow velocity shows the minimum value and the flow characteristic is irregular.

To compare the pitch angles of 44°, 59°, 64° with the suggested design the pressure difference and the flow rate of the pitch angle of 54°, impeller are shown in Fig. 9. The pressure difference and the flow rate of the pitch angle of 59° show the increase of 113%and 106% compared with those of the suggested design pitch angle of 59°, respectively. However, the pitch angle of 44° produces the lower static pressure rise and the lower flow rate that those of 54° design pitch angle due to the smallest the lower flow resistance at the leading edge. The pitch angle of 64°, cause the large decrease of static pressure and flow rate

V. Conclusion

The variation pitch angles of the impeller improving flow and static pressure of was analyzed to improve the flow rate and the static pressure of a turbo fan. After we analyzed effect of the pitch angle variation on the flow rate and static pressure, we reached the following conclusion.

1) By comparing the flow rate of 1,175 CMH, 1,270 CMH, 1,340 CMH, and 800 CMH of the each pitch angle of 44 °, 54°, 59°, and 64° respectively, the largest flow rate can be obtained by the pitch angle of 59°.
2) The static pressure difference between the impeller by the pitch angle variations of 44°, 54°, 59°, and 64° were, 120 Pa, 214 Pa, 242 Pa, and 60 Pa, respectively. The pitch angle 59° showed the highest static pressure.
3) In order to increase the flow rate and the static pressure of the axial flow turbo fan, the 59° of pitch angle should be adopted.

References

[1] Railly, J. W., 1984, Computational Methods in Turbomachinery, Mechanical Engineering Publications, London.
[2] Kim, K. Y., Kim, J. Y., and Chung, J. Y., 1997, Three-dimensional analysis of the flow through an axial-flow fan, Journal of KSME, Vol. 21, No. 4, pp. 541-542.
[3] Hur, N. K., Kim, U., Kang, S. H., 1999, A numerical study on cross flow fan : effect of blade shapes on fan performance, Journal of. KFMA, Vol. 2, No.1, pp. 96-102.
[4] Jorjensen, R., 1976, Fan engineering, Buffalo, New York, pp. 217-222.
[5] Lakshminarayana, 1996, "Fluid dynamics and heat transfer of turbomachinery", Wiley. Interscience, pp.358-362.
[6] Ryu, I. K., 2003, Studies on the airflow characteristics with revision of impeller design and the noise characteristics with arrangement of silencer in an axial turbo fan, Hanyang University, Seoul, Korea.
[7] Hirsch, C., 1988, "Numerical computation of internal and external flows", Vol. 1, Wiley.
[8] Patankar, S. V., 1980, Numerical heat transfer and fluid flow, McGraw-Hill, New York